Evaluation of Terrain Effects in Airborne Electromagnetic Surveys

MN1.6

Guimin Liu, Macquarie University, Australia; and Alex Becker, University of California, Berkeley*

SUMMARY

Terrain effects in airborne electromagnetic (AEM) surveys can be evaluated numerically using the boundary element method. It is found that modest valleys and hills do not affect the conventional estimates of apparent ground conductivity because the phase of the secondary field is largely unaffected by the topography. The attendant amplitude anomalies however can lead to erroneous estimates of the subsurface depth of the conducting ground when it is assumed to be covered by a resistive overburden. Topographic effects of features which are located at a distance greater than twice the flight altitude may be neglected.

INTRODUCTION

Terrain effects can be an important factor in any geophysical survey. They are of course most evident in gravity data and less so in magnetic data. They are not, however, usually observed in electromagnetic data and were, until recently, of no concern to the geophysicist who used electromagnetics for mineral exploration. Because of the high audio frequencies involved, electromagnetic terrain effects were first noticed in VLF data acquired in mountainous areas (Whittles, 1969). Further work on this topic by Karous (1979) and by Eberle (1981) offered a simple explanation for the observed terrain related VLF anomalies. These could be accounted for by applying Ampere's Law to an assumed uniform current concentration in a topographic protrusion (Karous, 1979) or, in special cases, by simply considering the reflection of plane waves from an inclined surface (Eberle, 1981).

Neither one of these methods allows the prediction of topographic effects for a closely coupled electromagnetic system such as is routinely used in ground and airborne electromagnetic (AEM) surveys. Typically, these surveys are usually done in the lower audio range (0.3-3 kHz) and such effects are not observed often. The use of electromagnetics however, was recently expanded from mineral exploration to emcompass geological mapping related to environmental, geohydrological and geotechnical problems (Fraser, 1978). Accordingly, conventional EM equipment was ameliorated to operate over a much wider frequency range (Fraser, 1979) so that at this point operation frequencies up to 50 kHz are available. One can thus expect that terrain effects will now be observed more commonly.

The objective here is to numerically evaluate the topographic effects in an AEM survey using the boundary element method (Brebbia et al., 1984). For eddy current problems, the theory of deriving the coupled boundary integral equations was given by Mayergoyz (1982). These equations have been known for some time in EM literature, yet no numerical results appear to have been presented based on this formulation. Here we transform the pertinent equations in the strike direction for two-dimensional (2-D) topography, and then solve the transformed equations numerically. Although in some aspects this work resembles that of Doherty (1988) or that of Parry and Ward (1971), it differs in the underlining principle used to derive the boundary integral equations. Furthermore, since in our case the EM field in the air is quasi-static, a scalar potential suffices to describe the magnetic field. The resulting boundary integral equations involve 25% fewer unknowns than used by Doherty so that the numerical computation is considerably faster. Following presentation of the theory, numerical results for topographic features such as valleys and hills will be shown.

METHOD OF COMPUTATION

Consider an alternating electric current loop (magnetic dipole) in the air above a conductive homogeneous ground with arbitrary surface relief. In the case examined, the height of the source over the ground is small compared with the wave length so that the electromagnetic fields are quasi-static. The secondary magnetic field in the air can be represented by an integral of fictitious magnetic charges ξ distributed on the ground surface. Similarly, the magnetic field in the earth can be represented by an integral of fictitious electric currents $\mathbf{J}$ distributed on the ground surface. From the continuity conditions of magnetic field, it can be shown that the charges and currents satisfy the following equations (Mayergoyz, 1982)

$$\mathbf{J}(M) + \frac{1}{2\pi}\int_s \mathbf{n}\times(\mathbf{J}(P)\times\nabla\frac{e^{-ikr}}{r_{PM}})\,ds - \frac{1}{2\pi}\int_s \xi(P)\,\mathbf{n}\times\nabla\frac{1}{r_{PM}}\,ds = -\frac{1}{2\pi}\mathbf{n}\times\mathbf{H}_p \qquad (1)$$

$$\xi(M) - \frac{1}{2\pi}\int_s \xi(P)\,\mathbf{n}\cdot\nabla\frac{1}{r_{PM}}\,ds + \frac{1}{2\pi}\frac{\mu}{\mu_0}\int_s \mathbf{n}\cdot(\mathbf{J}(P)\times\nabla\frac{e^{-ikr}}{r_{PM}})\,ds = -\frac{1}{2\pi}\mathbf{n}\cdot\mathbf{H}_p \qquad (2)$$

Here $\mathbf{n}$ is the unit normal at a field point M on ground surface S; $\mathbf{H}_p$ is the primary magnetic field at M; the gradient operator ∇ is for the field point M. All the integrals in equations (1) and (2) are in the sense of the Cauchy principal value. Once the charges are obtained, the secondary magnetic field at point O in the air can be computed by,

$$\mathbf{H}_s = \int_s \frac{\xi(P)}{r_{PO}^3}\mathbf{r}_{PO}\,ds \qquad (3)$$

If the topography is two-dimensional, equations (1) and (2) can be transformed into the wavenumber domain along the strike (y) direction. The fictitious current **J** has two components J_y and J_s on the surface S. Here J_y is the component along the y direction and J_s is the tangential component perpendicular to the y-direction. In the wavenumber k_y domain, let

$$\alpha_1(x, k_y) = \xi(x, k_y), \qquad \alpha_2(x, k_y) = J_y(x, k_y),$$
$$\alpha_3(x, k_y) = J_s(x, k_y);$$

then the equations for α_i (i=1,2,3) can be written as

$$\alpha_i(x, k_y) + \frac{1}{2\pi}\sum_{j=1}^{3}\left\{\int_{-\infty}^{+\infty} \alpha_j(x', k_y)\, f_{ij}(x,x',k_y)\, dx'\right\} = \frac{1}{2\pi}\beta_i(x,k_y) \qquad (i=1, 2, 3) \tag{4}$$

Here f_{ij} is the transformed kernel function, and β_i is the transformed primary magnetic field.

In order to solve the three coupled integral equations (4) numerically, the infinite integration interval must be truncated. This finite computational domain can then be discretized into N small elements with a node at the mid-point of each element. Integrating the contributions of every element in equation (4), we obtain a system of complex linear equations for the node values,

$$\mathbf{K}\,\alpha = \mathbf{B} \tag{5}$$

Here **K** is a 3Nx3N coefficient matrix assembled from the element integrals, α is a column vector of the unknown charge and current densities at all the nodes, and **B** is a column vector of the known boundary values on the surface S.

Equations (5) are solved independently for each of fifteen wavenumbers sampled on a logarithmic scale with five points per decade. Once the charge density is obtained, the horizontal and vertical components of the secondary magnetic field in the air can be computed in k_y domain from the Fourier transformation of equation (3). We now need to take the inverse Fourier transform to get the required final results. Prior to performing this operation however, the field values at logarithmically-spaced points in the k_y space need to be interpolated to a uniform grid using cubic spline interpolation.

VERIFICATION OF NUMERICAL RESULTS

An initial check of the numerical computation can be obtained by considering the case of a conductive half-space with a flat surface. In this case the analytical solution in a closed-form integral is well known (Ward and Hohmann, 1987) so that the numerical results can be verified for a wide range of frequencies. Our numerical results agree excellently with the analytical solution.

The numerical solution was also checked on a scale laboratory model of a valley. Aluminum was used to simulate the conductive terrain at a linear scale of 1:250. A model airborne electromagnetic system was built at the same scale and was " flown " at a field height of 10 m. The frequency scale of the model is 1:3750 while the conductivity scale is 2.34×10^8:1 . The system consisted of a co-planar, vertical axis transmitter and receiver, which were operated at a field frequency of 150 kHz (40 Hz in the laboratory) and were separated at a field distance of 10 m (4 cm in the laboratory). The conductivity of the aluminum used in our experiment is 2.34×10^7 S/m, which simulates a ground conductivity of 0.1 S/m. Note that the model parameters are related to the field parameters by the following equation (Frischknecht, 1987),

$$\sigma' f' l'^2 = \sigma f l^2 \tag{6}$$

Here σ, f, and l are the field conductivity, frequency and dimension while the primed quantities denote the corresponding model parameters.

The cross section of the simulated valley is a Gaussian function given by

$$t(x) = A \exp\left(-\frac{x^2}{0.361\, W^2}\right) \tag{7}$$

Here,

x = distance from the valley center line
t = topographic relief
A = valley depth
W = valley width at half A

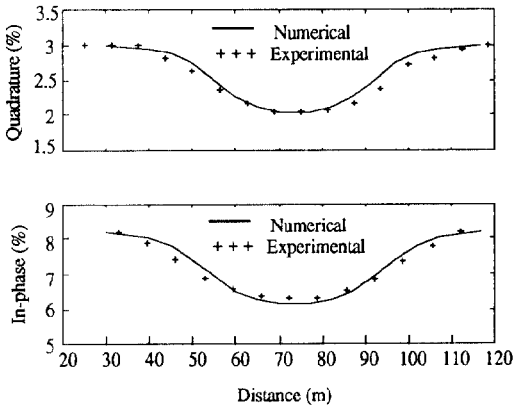

Figure 1. Comparison of numerical and experimental results for a valley model.

The shape of the valley is invariant along the strike direction. For the model valley, A and W were taken to be 3.4 m and 21 m respectively. The measurements and numerical calculation results for this model are displayed in Figure 1 which shows the in-phase and quadrature components of the secondary magnetic field. Here the system response is plotted at a point located mid-way between the transmitter and receiver. The measurement error in the experiment is estimated to be less than 5% for the in-phase component and 10% for the quadrature component. As shown in Figure 1, the numerical results and experimental data agree well.

TERRAIN EFFECTS

Let us now examine the numerical simulation results for the two common cases of a valley and a hill. The computations were done for a conventional co-axial helicopter borne AEM system operating at 8 kHz with a coil separation of 6.5m. While modern systems usually carry both the co-axial and co-planar coil systems we have found that the terrain effects in both cases are similar so that we will restrict our discussion to the co-axial case. The ground conductivity is taken as 0.1 S/m.

The first simulation is done for an overflight of a symmetric triangular valley with 20^0 side slopes and a base width of 120m. The system flight height is maintained at a constant barometric altitude of 30m above the flat terrain. In this case, as shown in Figure 2, both the in-phase and quadrature components of the secondary field show a negative anomaly over the valley. Its amplitude is about 100 ppm in the in-phase component and about 85 ppm in the quadrature secondary field.

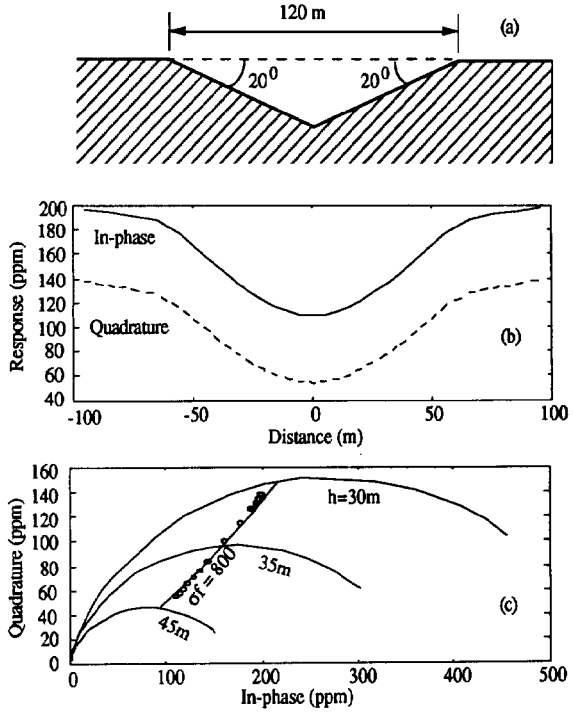

Figure 2. (a) model valley, (b) Numerical AEM response over the model valley, (c) Argand diagram of the response (circles); background lines are the AEM response over a flat ground surface.

To examine the effects of this topographic anomaly on the conventional method of data interpretation in terms of an apparent resistivity and depth to the conducting horizon (Fraser, 1978), we have replotted the profile data on an Argand chart of conductive half space response. As can be seen in Figure 2(c), the data points are very closely aligned with the σf = 800 radial. Given the 8 kHz frequency for the numerical experiment, all the data for this profile will yield the correct apparent resistivity of 0.1 S/m. The presence of the valley however is clearly indicated by the incorrect estimate of the system height above the conducting surface. This quantity turns out to be 43 m over the deepest portion of the valley which in fact lies at about 52m below the AEM system. Numerical experiments at other frequencies (1 and 64 kHz) yield similar results.

We next examine the numerical results that would be obtained in the overflight of a small, symmetric, triangular hill with a base width of 60 m and slopes of 20^0 . In this case the aircraft altitude is maintained at 30 m above the terrain including the hill summit which rises 11m above the background. The results for this simulation are shown in Figure 3. This time the signal amplitude rises somewhat as we approach the hill and then falls sharply when the aircraft altitude is raised to maintain constant terrain clearance over the hill top. Once again when the numerical results are plotted on the appropriate Argand diagram a correct value of apparent resistivity is indicated all along the profile. The apparent system terrain clearance however is in error as it indicates a system altitude of 35 m over the hill top.

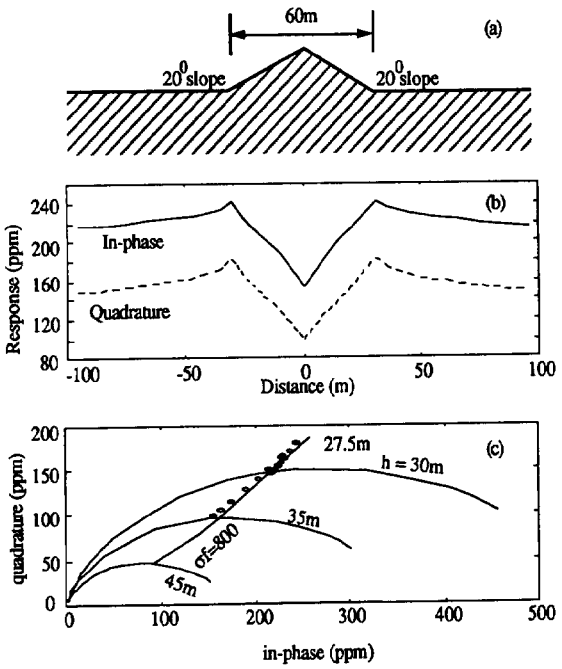

Figure 3. (a) model hill, (b) Numerical AEM response over the model hill, (c) Argand diagram of the response (circles); background lines are the AEM response over a flat ground surface.

CONCLUSIONS

The numerical results show that, conventional interpretation of the ground conductivity is not affected by topographic features such as valleys or hills. For a survey made over a valley, the AEM response will show a negative anomaly. The AEM response will also show a negative anomaly over a hill if the survey is draped (distance between the system and the ground surface is kept constant). In all these cases, the effects of the topographic features may be neglected at lateral distances greater than twice the system altitude. This can be expected by noting that the

footprint for any AEM system is of the order of the system altitude.

Although the algorithm presented here is developed for a conductive topography it can be also applied to modeling the effects of a conductive basement under a resistive overburden of varying thickness. Another application of the present algorithm is for determining ice thickness in many areas of the Arctic.

REFERENCES

Brebbia, C. A., Telles, J. C. F., and Wrobel, L. C., 1984, Boundary element techniques - theory and applications in engineering: Springer-Verlag.

Doherty, J., 1988, EM modeling using surface integral equations, Geophysical Prospecting, vol. 36, 644-668.

Eberle, D., 1981, A method of reducing terrain relief effects from VLF-EM data, Geoexploration, vol.19, 103-114.

Fraser, D. C., 1978, Resistivity mapping with an airborne, multicoil, electromagnetic system: Geophysics, vol.43, 144-172.

Fraser, D. C., 1979, The multicoil II airborne electromagnetic system: Geophysics, vol. 44, 1367-1394.

Frischknecht, F.C., 1987, Electromagnetic physical scale modeling, in Nabighian, M.N. Ed., Electromagnetic methods in applied geophysics-theory, Vol.1.

Karous, M.R., 1979, Effects of relief in EM methods with very distant source, Geoexploration, vol.17, 33-42.

Mayergoyz, I. 1982, Boundary integral equations of minimum order for the calculation of three-dimensional eddy current problems, IEEE Trans. on Magnetics Mag-18, 536-539.

Parry, J. R., and Ward, S. H., 1971, Electromagnetic scattering from cylinders of arbitrary cross-section in a conductive half-space: Geophysics, vol. 36, 67-100.

Ward, S.H., and Hohmann, G.W., 1987, Electromagnetic theory for geophysical applications, in Nabighian, M.N. Ed., Electromagnetic methods in applied geophysics-theory, Vol.1.

Whittles, A.B.L., 1969, Prospecting with radio frequency EM-16 in mountainous regions, Western Miner, vol.42, 51-56.